



Potential biological damage of human peripheral blood lymphocytes induced by computed tomography examination of the oromaxillofacial region

Pan Yang, DDS, PhD,^a Shuo Wang, DDS,^a Denggao Liu, MD,^a Hua Zhao, DDS, PhD,^b Qingjie Liu, DDS, PhD,^b and Gang Li, DDS, PhD^a

Objectives. The aim of this study was to examine whether oromaxillofacial computed tomography (CT) examination causes biologic damage in lymphocytes and whether the biologic damage is related to radiation dose, patient age, or gender.

Study Design. Peripheral blood was taken from 51 individuals and divided into control, in vivo, and in vitro irradiation groups. Biologic damage was assessed by comparing rates of chromosomal aberrations (CAs), including dicentric chromosomes (dics), centric rings, and acentric fragments; and nuclear aberrations, including micronuclei (MN), nuclear buds (NBUDs), and nucleoplasmic bridges (NPBs) in the peripheral blood before and after CT examination. Absorbed and effective doses were calculated with the software VirtualDose, and the blood dose was estimated accordingly.

Results. The rates of acentric fragments, MN, NBUDs, and NPBs in the in vivo ($P \leq .008$) and in vitro ($P \leq .003$) irradiation groups were significantly higher than those in the control groups. The acentric fragment rate ($P = .013$) and MN rate ($P = .002$) were higher in the in vitro group than in the in vivo group. There was no correlation between change rates of CAs and nuclear aberrations with radiation dose. Positive correlations of MN rates with age were found in all groups ($\rho \geq 0.590$).

Conclusions. Certain doses of radiation in oromaxillofacial CT examination may induce CAs and nuclear aberrations in lymphocytes. (Oral Surg Oral Med Oral Pathol Oral Radiol 2020;130:708–716)

Examination of patients with computed tomography (CT) is necessary and commonly used for diagnosis, treatment planning, and prognosis evaluation in daily clinical work. With increased use of CT examinations, potential biologic damage has become a public concern.

Chromosomal aberration (CA) is the outcome most often used to evaluate the potential biologic damage to human beings in relation to ionizing radiation exposure. Different types of CAs are observed in exposed lymphocytes, including dicentric chromosomes (dics), centric rings, and acentric fragments. Dics are abnormal chromosomes with 2 centromeres. They are formed by the incorrect combination of 2 broken chromosomes, resulting in fragments without centromeres. The centric ring is formed from the incorrect rejoining of a chromosome when 2 breaks occur on either side of the centromere in the same chromosome. The acentric fragment is a piece of a broken chromosome of varying size and does not contain a centromere. Acentric fragments may be produced separately or in association with dics and centric rings.¹ Dics are unstable because their frequency decreases with the turnover of peripheral blood lymphocytes. Thus, for reliable dose assessment of all 3 abnormalities, CA assays should be performed within a few weeks of exposure to radiation.²

Nuclear aberrations representing chromosomal damage and genomic instability also result from radiation exposure and are assessed with the cytokinesis-block micronucleus (CBMN) assay.^{3,4} These aberrations include micronuclei (MN), nuclear buds (NBUDs), and nucleoplasmic bridges (NPBs). MN are considered to be indicators of chromosome loss and chromosome breakage.⁵ They are formed by an acentric fragment or chromatid fragment that lags in the anaphase of cell division, ending up in the cellular cytoplasm and not in the nucleus.² NBUDs are generated to eliminate amplified DNA and DNA repair complexes. NPBs are formed from dicentric chromosomes during anaphase, when the centromeres are pulled to opposite poles.⁶

Because nuclear aberrations can only be expressed in cells that have completed nuclear division, the CBMN assay has been developed to identify such cells on the basis of their binucleated appearance when performing cytokinesis blocked by cytochalasin B, a microfilament-assembly inhibitor. The CBMN assay is now widely used in monitoring genotoxicity caused by physical and chemical factors and in screening the radiosensitivity of tumors and interindividual variations.⁵

The radiation dose in CT examinations can be estimated by applying several parameters. Among those, the

^aDepartment of Oral and Maxillofacial Radiology, Peking University School and Hospital of Stomatology, Beijing, China.

^bChina CDC Key Laboratory of Radiological Protection and Nuclear Emergency, National Institute for Radiological Protection, Chinese Center for Disease Control and Prevention, Beijing, China.

12 March 2020/26 May 2020 © 2020 Elsevier Inc. All rights reserved. 2212-4403/\$-see front matter

<https://doi.org/10.1016/j.oooo.2020.05.013>

Statement of Clinical Relevance

Computed tomography (CT) examination of the oromaxillofacial region can cause nuclear damage in the peripheral lymphocytes. Although CT is very helpful in medical care, this potential risk must be borne in mind when prescribing the examination.

CT dose index (volume) ($CTDI_{vol}$) and the dose–length product (DLP) are widely used. However, both $CTDI_{vol}$ and DLP are indices of the radiation output of the CT system, and neither of them corresponds directly with the radiation dose delivered to the patient.⁷ Because it is not possible to measure the doses delivered to a patient directly, a human simulation phantom is often used for the purpose of measuring the doses absorbed by various organs. This method is time consuming and not a real measurement. A practical method for a relatively accurate estimation of absorbed doses and, consequently, the calculated effective dose (E), can be performed by using the Monte Carlo (MC) method.^{8–10}

To our knowledge, no studies have exclusively investigated the possible biologic damage resulting from CT examination of the oromaxillofacial region. Therefore, the objectives of the study were to assess whether exposure of blood cells (in vivo and in vitro) to radiation in doses used in CT examinations increases the formation of CAs and nuclear aberrations; to examine the correlations between radiation dose and the production of CAs and nuclear aberrations; and to examine the correlations between patient age or gender and the formation of these anomalies. The null hypotheses stated that there would be no significant effect of CT radiation doses on the frequency of CAs and nuclear aberrations and no significant relationship between radiation dose, patient age, or patient gender and the production of these abnormalities.

MATERIALS AND METHODS

Patients

Patients in the study were selected from approximately 1500 patients who had had CT examinations of the head and neck in our hospital from May to September 2019. The inclusion criteria were as follows:

1. No major systemic diseases, including diseases of blood
2. No history of cancer and/or radiation therapy
3. No history of surgical treatment
4. No history of systemic medication
5. No recent infections
6. No exposure to diagnostic radiation within the past three months
7. No current history of smoking and/or drinking

In total, 51 patients were included. All CT examinations and blood collections were performed on the basis of treatment requirements and not solely for the purposes of this research.

Before CT examination, individual patient information, including age, gender, height, weight, medical history, radiographs exposed, and the exposure parameters, was recorded. The study was approved by the

Institutional Review Board of the Peking University School and Hospital of Stomatology, (Beijing, China) and conducted in compliance with the tenets of the Helsinki Declaration. All procedures were performed in accordance with the relevant guidelines and regulations. Each patient included in the project signed a detailed informed consent form.

CT examination and blood sample collection

CT examination was performed with a 16-slice helical CT scanner (Optima CT 520; GE Healthcare, Waukesha, WI). Before the CT examination, the accuracy and repeatability of the $CTDI_{vol}$ of the machine was verified. During the CT examination, the tube voltage was set at 120 kVp, and the tube current was automatically adjusted according to the patient's condition, resulting in a range of 80 mA to 300 mA. The other imaging parameters included rotation time of 0.8 second, table feed per rotation of 18.75 mm, detector width of 1.25 mm, scan field of view of 25 cm, and matrix of 512 mm. The collimation (beam width) of the CT scan was 20 mm, according to the manufacturer's setting, and the pitch was 0.938. Scanning length was 14 cm to 23.75 cm.

Before the CT examination, a 4mL sample of peripheral blood was drawn from each patient, of which 2 mL of blood was used for the control group and 2 mL for the in vitro irradiation group. For in vitro irradiation, the blood collection tube was placed beside the patient's head during exposure in the CT examination. To ensure that the 3-dimensional space between the blood collection tube and the x-ray tube remained consistent, the blood collection tube was placed close to the left inner wall of the head positioning device and the long axis of the tube paralleled the Z-axis, making the midpoint through the X-axis of the positioning line. After 5 minutes of the examination, 2 mL of blood was retaken from the same patient and was used for the in vivo irradiation group.

Peripheral blood lymphocyte cultures for CA assay

Whole blood (0.5 mL) from each of the 3 groups (control, in vivo irradiation, and in vitro irradiation) was added to 4.5 mL of polyhydroxyalkanoates (PHA)–containing medium (Biological Industries, Kibbutz Beit Haemek, Israel). After stimulation with PHA for 68 hours, colchicine solution (Coolaber, Beijing, China) was added 4 hours before harvesting. After hypotonic treatment with 0.075 M potassium chloride, lymphocytes were fixed in a methanol-to-acetic acid ratio of 3:1, and the cell suspension was dropped onto clean glass slides. Slides were stained with 10% Giemsa stain and then microscopically observed under $\times 1000$ oil immersion (Olympus BX51, Tokyo, Japan). Scoring for the presence of CAs was performed blindly by 2 trained, experienced observers, who were

not informed of the irradiation status before evaluation. These observers each had greater than 5 years of experience in microscopic examination. For each slide, 200 well-spread metaphases were scored. Each metaphase was evaluated for the presence of dics, centric rings, and acentric fragments. To ensure correct scoring, only those dics or centric rings that were observed together with fragments were counted. These fragments were not included in the scoring of acentric fragments.

Peripheral blood lymphocyte cultures for CBMN assay

Whole blood (0.5 mL) from each of the 3 groups (control, in vivo irradiation, and in vitro irradiation) was added to 4.5 mL of PHA-containing medium. After stimulation with PHA for 44 hours, cytokinesis was blocked with 6 $\mu\text{g}/\text{mL}$ cytochalasin B (Cyt B; Alladin, Shanghai, China) and lymphocytes were harvested 28 hours later. The hypotonic treatment and fixing and staining procedures were the same as for the CA assay. Slides were examined under an optical microscope at $\times 400$ magnification and scored by the 2 observers. In total, 2000 binucleated lymphocytes for each subject were examined for MN, NBUDs, and NPBs, according to the scoring criteria outlined by the Human Micronucleus Project.¹¹

Dose calculation

CTDI_{vol} and DLP were recorded from the CT system. The absorbed dose and E were calculated by using VirtualDose (Virtualphantoms Inc., Albany, NY). E was calculated by using tissue weighting factors from the International Commission on Radiological Protection publication No. 103.¹² The blood absorbed doses were estimated as recommended by Rothkamm et al.¹³ Organ-specific blood volumes were adopted from previously reported reference data.¹⁴ Gender-specific blood volumes and radiation dose calculations were averaged. The blood-weighted dose (estimated blood dose by organ-specific blood volumes) is the absorbed dose in each organ or tissue multiplied by the proportion of blood. The blood absorbed dose is the sum of the blood-weighted doses for all organs or tissues (i.e., the absorbed dose in each organ or tissue multiplied by the proportion of blood volume). Estimated blood dose by organ-specific blood volumes (the blood-weighted dose) is shown in Table I.

Statistical analysis

The software package SPSS version 16.0 for windows (SPSS Inc., Chicago, IL) was employed for statistical analysis. Differences between the mean aberration detection rates of dics, centric rings, acentric fragments, MN, NBUDs, and NPBs in blood drawn before and after CT examinations were analyzed by using Wilcoxon's signed rank test. Friedman's signed rank

Table I. Estimated radiation doses in blood calculated with phantom dosimetry

Organ	Blood volume (100%)*	Blood absorbed dose (mGy)	Blood-weighted dose (mGy)
Adrenal glands	0.1	0.06	0.0001
Bladder	0	0.08	0
Brain	1.2	2.1	0.0252
Gonads	0	0.01	0
Heart	16	0.66	0.1056
Kidneys	2	0.04	0.0008
Liver	10	0.08	0.0080
Lung	12.5	0.78	0.0975
Muscle	12.25	0.37	0.0453
Esophagus	0.1	1.79	0.0018
Pancreas	0.6	0.11	0.0007
Skin	3	0.44	0.0132
Small intestine	3.8	0.01	0.0004
Spleen	1.4	0.1	0.0014
Stomach	0.9	0.11	0.0010
Thyroid	0.1	4.58	0.0046
Skeleton	7	0.83	0.0581
Lymph nodes	0.2	0.39	0.0008
Fat	6.75	0	0
Large intestine	2.2	0.01	0.0002
large veins	18	0	0
All other tissues	1.9	1.63	0.0310
All organs	100	...	0.3956

*Contribution of blood in given organ to total blood volume.

test was used to analyze the differences among the 3 sets of sample groups (control, in vivo irradiation, and in vitro irradiation groups). The change rates, defined as the rate of aberrations in the in vivo or in vitro group minus the rate in the control group, were examined for correlation between aberrations and radiation doses. For analysis of correlations among different dose levels, the change rates of CAs and the nuclear aberrations, and correlations between patient age and gender and the rates of CAs and nuclear alterations, Spearman's rank correlation test was employed. The significance of differences was set at $P < .05$.

RESULTS

Patients

The study included 30 males and 21 females. The age of the patients (mean \pm standard deviation [SD]) was 40.76 ± 13.43 years. The regions exposed during CT ranged from the calvarium to the thyroid gland (2 cases); from the forehead to the thyroid gland (13 cases); from the calvarium to the clavicle (1 case); from the eyebrows to the thyroid gland (30 cases); from the eyebrows to the clavicle (3 cases); and from nasion to the thyroid gland (2 cases).

Radiation exposure and aberrations

Chromosomal aberrations. Cytologic examples of CAs are shown in Figure 1. Aberration data from the

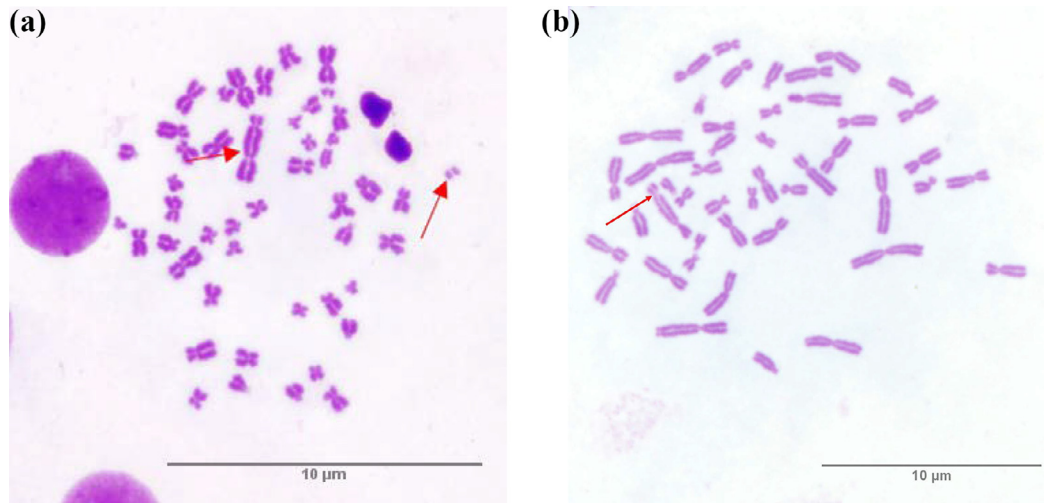


Fig. 1. Chromosomal aberrations. Dicentric chromosomes (dic) and acentric fragments, indicated by the arrows, were observed in the blood samples. No centric rings were detected. **A**, Dicentric chromosomes (dic). **B**, Acentric fragments.

CA assay are shown in Table II. Compared with the control group, the overall CA rates of both the in vivo ($P = .005$) and the in vitro ($P < .001$) irradiation groups were significantly increased. The mean rates of dics and acentric fragments in the in vivo irradiation group were greater than in the control group, and the rates in the in vitro irradiation group were greater than in the in vivo group. No centric rings were detected in any of the 3 groups.

For dics, the differences in rates of aberrations among the 3 groups (control, in vivo irradiation, and in vitro irradiation groups) were not significant. Comparisons of pairs of conditions yielded insignificant differences (control vs in vivo: $P = .317$; in vivo vs in vitro: $P = .564$; and in vitro vs control: $P = .157$). For acentric fragments, however, the differences in the rates of aberrations among the 3 groups were significant, with comparisons of pairs of conditions also being significant (in vivo significantly larger than

control: $P = .008$; in vitro significantly larger than in vivo: $P = .013$; and in vitro significantly larger than control: $P < .001$). The results are shown in Figure 2.

Nuclear aberrations. Cytologic examples of MNs, NBUDs, and NPBs are shown in Figure 3. Aberration data from the CBMN assay are shown in Table III. The rates of all 3 types of aberrations were higher in the in vivo irradiation group than in the controls, and higher in the in vitro group than in the in vivo group. Compared with the control group, the overall nuclear aberration rates of both in vivo ($P < .001$) and in vitro ($P < .001$) were significantly increased. For MN, the differences in rates of aberrations among the 3 groups (control, in vivo irradiation, and in vitro irradiation groups) were significant. Comparisons of pairs of conditions were also significant, with the rate of MN in the in vivo irradiation group larger than in the controls ($P < .001$); the rate in the in vitro group larger than in the in vivo group ($P = .002$); and the rate in the in vitro group larger than in the control group ($P < .001$). For NBUDs and NPBs, comparisons were significant between the in vivo and control groups ($P \leq .018$) and between the in vitro and control groups ($P \leq .003$), but there were no significant differences between the in vivo and in vitro groups ($P \geq .440$), as shown in Figure 4. The overall mean rates of MN, NBUDs, and NPBs in the in vivo and in vitro irradiation groups were higher than those in the control group and were significantly different among the 3 groups: MN ($P < .001$); NBUDs ($P = .002$); and NPBs ($P = .010$).

Table II. Cells observed, detection numbers of each type of aberration, detection number of total aberrations, and detection rate of mean aberration for chromosomal aberrations in the CA assay

	Control	In vivo irradiation	In vitro irradiation
Cells observed	10200	10200	10200
Dicentric chromosomes	0	7	22
Centric rings	0	0	0
Acentric fragments	0	1	2
Total aberration	0	8	24
detection number			
Mean aberration	0	0.08	0.24
detection rate (%)			

CA, chromosomal aberration.

Correlations of radiation dose with aberrations

The ranges of $CTDI_{vol}$, DLP, E, and blood absorbed dose are shown in Table IV. The blood absorbed doses

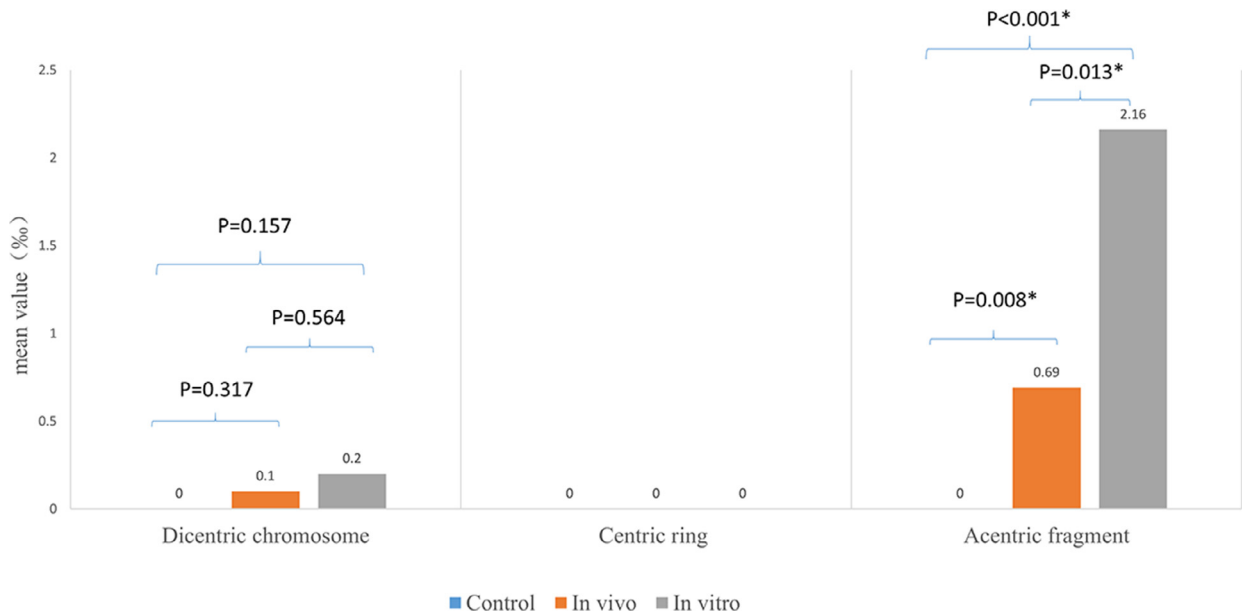


Fig. 2. Mean rates of dicentric chromosomes, centric rings, and acentric fragments in the control group and in the in vivo and in vitro irradiation groups. *Statistically significant difference.

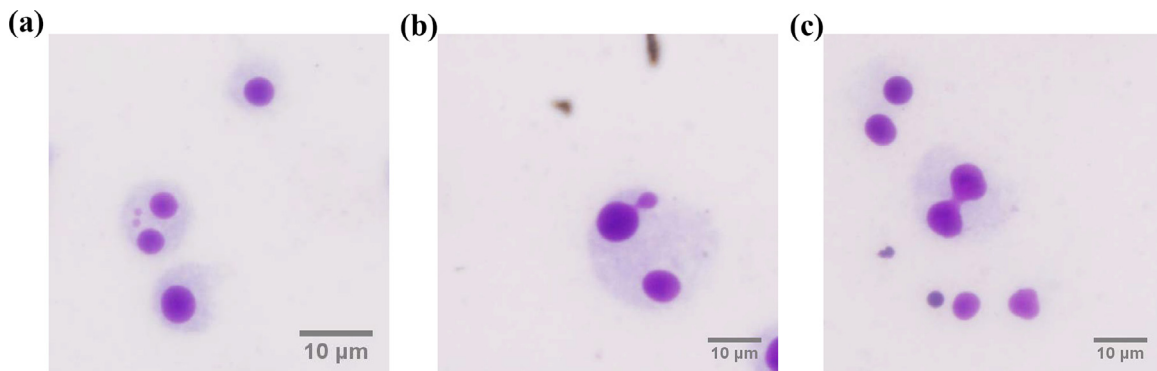


Fig. 3. Nuclear aberrations. A, Micronuclei. B, Nuclear buds. C, Nucleoplasmic bridges.

were estimated with phantom dosimetry and ranged from 0.24 mGy to 0.83 mGy.

There was no correlation between irradiation doses and the change rates of CAs ($P \geq .110$) and nuclear aberrations ($P \geq .222$) in the in vivo and in vitro irradiation groups. The correlation coefficients and the P values are shown in Table V and Table VI.

Correlations of age and gender with aberrations

Neither age nor gender had a correlation with CAs before or after CT examination either for the in vivo ($P \geq .365$) or the in vitro ($P \geq .088$) irradiation groups (Table VII). Positive correlations of MN rates with age were found in the control ($\rho = 0.629$; $P < .001$), in vivo ($\rho = 0.590$; $P < .001$), and in vitro ($\rho = 0.624$; $P < .001$) irradiation groups. However, there were no correlations between age and NBUDs or NPBs ($P \geq .057$). There were no correlations between gender and

any of the nuclear aberrations before or after CT examination ($P \geq .073$) (Table VIII).

DISCUSSION

Analysis of CAs in human peripheral blood lymphocytes has been developed as an indicator of ionizing radiation dose.¹ In the present study, the total CA mean aberration detection rate was significantly increased after CT examination ($P \leq .005$). This is in line with the findings of the study by Kanagaraj et al., in which the overall mean CA frequency obtained after CT examination showed an extremely significant increase compared with that obtained before exposure.¹⁵ In our study, the acentric fragment rates in the in vivo and in vitro irradiation groups, compared with that in the control group, were significantly increased ($P \leq .008$), similar to the findings by Stephan et al., who analyzed the peripheral blood of 10 children after CT

Table III. Cells observed, detection number of each type of aberration, detection number of total aberrations, and detection rate of mean aberration for nuclear aberrations in the CBMN assay

	Control	In vivo irradiation	In vitro irradiation
Cells observed	102000	102000	102000
Micronuclei	746	1135	1323
Nuclear buds	7	20	25
Nucleoplasmic bridges	19	37	49
Total aberration detection number	772	1192	1397
Mean aberration detection rate (%)	0.76	1.17	1.37

CBMN, cytokinesis block micronuclei.

examination and found that the acentric fragment rate had increased significantly.¹⁶

Another finding of the present study was that the mean aberration detection rate of dics was not significantly increased in the in vivo or in vitro irradiation group compared with the control group ($P \geq .157$). This contrasts with results from other studies. Stephan et al.¹⁶ conducted a small-scale investigation with samples from 10 pediatric patients undergoing CT examination (blood doses in the range of 1.2–31.3 mGy). They found that single CT scans significantly elevated dic formation in the peripheral lymphocytes of children 0.4 to 9 years of age but not in those of children 10 to 15 years of age, indicating that younger children may be more radiosensitive compared with older patients. In 2015, Abe et al.¹⁷ analyzed CAs in 10 children with lymphoma, lung cancer, and abnormal

Table IV. Descriptive data for computed tomography dose index (volume), dose–length product, effective dose, and blood absorbed dose from 51 patients

	Minimum	Maximum	Mean	Standard deviation
CTDI _{vol} (mGy)	25.26	44.21	33.76	4.57
DLP (mGy·cm)	446.25	917.10	661.90	130.48
E (mSv)	0.39	1.06	0.60	0.12
Blood absorbed dose (mGy)	0.24	0.83	0.39	0.10

CTDI_{vol}, computed tomography dose index (volume); DLP, dose–length product; E, effective dose.

chest shadows after CT examination and found that dics were significantly increased, but the increased dic values were not correlated with the radiation dose. In that study, the DLP per CT examination was 619.1 to 5501.3 mGy·cm and the E range was 5.78 to 60.27 mSv. In the study by Shi et al.,¹⁸ dics were significantly increased in 60 patients without cancer who underwent cardiac or hepatic dynamic CT examinations. The DLP range of these CT examinations was 629.0 to 3171.9 mGy·cm, and the E range was 8.8 to 44.4 mSv. The possible explanation for the differences between these investigations and the present study may be attributed to the fact that the formation of dics is not sensitive at very low doses. In the present investigation, DLP (446.25–917.10 mGy·cm) and E (0.39–1.06 mSv) were lower than the radiation doses reported in the studies mentioned above.^{16,17}

The CBMN assay has been established to quantify radiation effects on chromosomal DNA. In the present study,

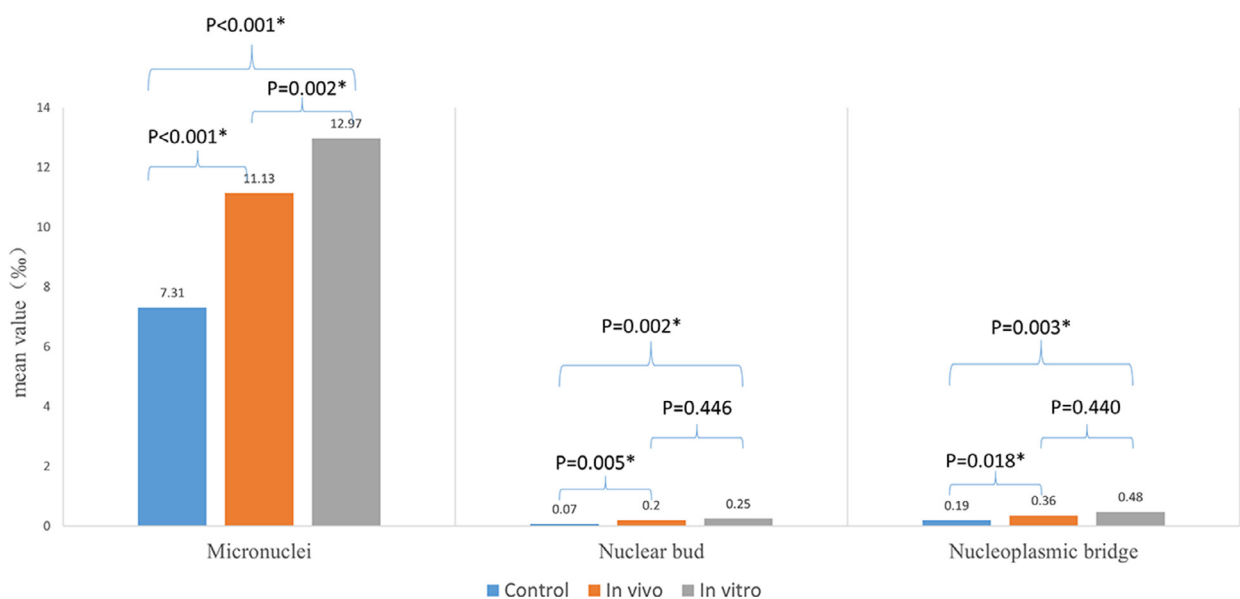


Fig. 4. Mean rates of micronuclei, nuclear buds, and nucleoplasmic bridges in the control group and in the in vivo and in vitro irradiation groups.

Table V. P values and ρ from Spearman’s rank correlation test for the relationship between radiation dose and the change rates of dicentric chromosomes, centric rings, and acentric fragments

		<i>Dic change rate</i>		<i>Centric ring change rate</i>		<i>Acentric fragment change rate</i>	
		<i>In vivo</i>	<i>In vitro</i>	<i>In vivo</i>	<i>In vitro</i>	<i>In vivo</i>	<i>In vitro</i>
CTDI _{vol}	ρ	0.257	0.062	–	–	0.003	–0.141
	P value	.110	.702	–	–	.984	.397
DLP	ρ	0.104	0.035	–	–	0.115	–0.075
	P value	.523	.832	–	–	.481	.647
Blood absorbed dose	ρ	0.041	0.139	–	–	0.012	0.036
	P value	.781	.342	–	–	.933	.806

CTDI_{vol}, computed tomography dose index (volume); *Dic*, dicentric chromosomes; *DLP*, dose–length product.

Table VI. P values and ρ from Spearman’s rank correlation test for the relationship between radiation dose and the change rates of MN, NBUDs, and NPBs after radiation

		<i>MN change rate</i>		<i>NBUD change rate</i>		<i>NPB change rate</i>	
		<i>In vivo</i>	<i>In vitro</i>	<i>In vivo</i>	<i>In vitro</i>	<i>In vivo</i>	<i>In vitro</i>
CTDI _{vol}	ρ	–0.113	0.006	0.083	0.197	0.046	0.152
	P value	.487	.969	.611	.222	.780	.348
DLP	ρ	–0.062	0.077	0.017	0.133	0.002	0.164
	P value	.705	.636	.919	.413	.989	.311
Blood absorbed dose	ρ	–0.028	0.009	0.152	–0.028	0.063	0.120
	P value	.848	.949	.297	.848	.668	.411

CTDI_{vol}, computed tomography dose index (volume); *DLP*, dose–length product; *MN*, micronuclei; *NBUD*, nuclear bud; *NPB*, nucleoplasmic bridge.

Table VII. P values and ρ from Spearman’s rank correlation test for the relationship between patient age and gender and the rates of dicentric chromosomes, centric rings, and acentric fragments

		<i>Dicentric chromosome</i>			<i>Centric ring</i>			<i>Acentric fragment</i>		
		<i>Control</i>	<i>In vivo</i>	<i>In vitro</i>	<i>Control</i>	<i>In vivo</i>	<i>In vitro</i>	<i>Control</i>	<i>In vivo</i>	<i>In vitro</i>
Age	ρ	–	0.010	0.017	–	–	–	–	–0.087	–0.163
	P value	–	.947	.905	–	–	–	–	.543	.253
Gender	ρ	–	–0.118	0.241	–	–	–	–	0.129	–0.010
	P value	–	.408	.088	–	–	–	–	.365	.944

no statistical results.

Table VIII. P values and ρ from Spearman’s rank correlation test for the relationship between age/gender and the rates of MN, NBUDs, and NPBs

		<i>MN</i>			<i>NBUD</i>			<i>NPB</i>		
		<i>Control</i>	<i>In vivo</i>	<i>In vitro</i>	<i>Control</i>	<i>In vivo</i>	<i>In vitro</i>	<i>Control</i>	<i>In vivo</i>	<i>In vitro</i>
Age	ρ	0.629	0.590	0.624	–0.103	–0.269	–0.050	–0.061	0.179	0.014
	P value	< .001*	< .001*	< .001*	.473	.057	.726	.668	.209	.924
Gender	ρ	0.155	0.184	0.209	–0.184	–0.161	–0.254	0.083	0.176	0.035
	P value	.279	.195	.142	.196	.259	.073	.562	.217	.806

MN, micronuclei; *NBUD*, nuclear bud; *NPB*, nucleoplasmic bridge.

*Significant difference at $P < .05$.

MN mean aberration detection rates after CT examination were significantly different from those before the examination ($P < .001$), which is the same as the results from the other studies.^{15,19} Ait-Ali et al.¹⁹ demonstrated that median

MN values increased significantly after radiologic procedures, with a median lifetime cumulative E of 7.7 mSv per patient (range 4.6–41.2 mSv) in children with congenital heart disease. In the study by Kanagaraj et al.,¹⁵ 27 patients

underwent CT examinations. The DLP range was 515.9 to 3726.9 mGy-cm, and the E range was 1.18 to 63.36 mSv. The results showed that the micronuclei cell rate was significantly increased after CT examination.

The results of the present study revealed that the CA and nuclear aberration rates in the in vitro group were higher than those in the in vivo irradiation group. This is because in the in vivo irradiation group, blood was not fully irradiated; soft tissues and bone had an attenuation effect on the radiation. Blood in the in vitro irradiation group, however, was completely exposed to radiation, with no attenuation effects.

Although CAs and nuclear aberrations in peripheral blood can be observed in healthy people, their numbers are much lower than in those exposed to radiation. This was identified in one of our previous studies,²⁰ in which 98 patients underwent cytogenetic examination of buccal mucosal cells before and 10 days after diagnostic dental radiographic procedures were performed. Of these patients, 8 were recalled 1.5 years later, not having had any additional irradiation during that period, and again had buccal mucosal cells collected for cytogenetic observation at the day of the examination and 10 days later. The mean aberration detection rate of MN in the 8 returning patients ranged from 0.5% for the first sampling at the 1.5 year recall examination down to 0.25% for the second sampling 10 days later. However, in the total of 98 patients, the mean rate of MN increased from 0.38% before irradiation to 0.60% immediately after dental radiographic examinations. To avoid the differences between individuals in the production of CAs and nuclear aberrations in normal conditions, the change rate of aberrations, which equals the mean aberration detection rate after CT examinations minus the rate before CT examinations, was used for the analysis of correlations with the radiation dose in the present study. No correlations were found between the irradiation doses and the change rates of CAs ($P \geq .110$) and nuclear aberrations ($P \geq .222$) in the present investigation. This is in line with the results from other research. In the study by Abe et al.,¹⁷ the correlation between the increment of dic formation and the effective radiation dose was analyzed but showed a negative result. In the study by Ait-Ali et al.,¹⁹ the same result was found, even taking the patient's weight into account when analyzing the relationship between the dose-area product and increased MN rates.

Age may play a role in DNA damage before and after irradiation. In the present study, the mean aberration detection rate of MN in human peripheral blood lymphocytes was positively correlated with age ($\rho \geq 0.590$, $P < 0.001$). One other study²¹ showed the same result. However, in our previous studies, age was not observed as a factor for the increased rate of MN in exfoliated oral mucosal cells.^{20,22} A possible explanation for this interesting finding may be that peripheral

blood lymphocytes are more sensitive to age changes²³ compared with exfoliated cells of the buccal mucosa.

Gender may also be one of the factors influencing DNA damage after irradiation. Studies have shown that MN frequency was higher in females than in males^{23,24}; however, this was not identified in the present research. The possible reason may be the low doses delivered to our study patients compared with the other investigations. For example, in the study by Cai et al., 2 Gy γ -ray photons were used. Further research is needed to address this problem. In addition, some studies have suggested that smoking and drinking may affect the frequency of MN and CAs.^{25,26} Therefore, patients who smoked or drank alcohol were excluded in the present study.

This study had some limitations. Changes in peripheral blood lymphocytes were monitored only 5 minutes after CT examination. First, we did not have sufficient time to observe the reparability of, and the long-term effects of radiation in, the human body, so we do not know whether the biologic effects continued to exist after 0.5 hours, 6 hours, or a longer time. Second, even though we calculated the patients' absorbed doses by using the VirtualDose software program, it is still a calculation based on 25 virtual phantoms, not real patients. The patients' individual conditions could not be completely or accurately reflected.

CONCLUSIONS

Radiation during CT examinations of the oromaxillofacial region can cause biologic damage in peripheral blood lymphocytes. Although CT of this region is very helpful in medical care, health care providers must bear in mind the potential risk when prescribing this examination.

FUNDING

This work was supported by the National Natural Science Foundation of China (No. 81671034)

REFERENCES

1. Lloyd DC, Dolphin GW. Radiation-induced chromosome damage in human lymphocytes. *Br J Ind Med.* 1977;34:261-273.
2. International Atomic Energy Agency (IAEA). Cytogenetic analysis for radiation dose assessment [R]. IAEA Technical Reports Series No. 405. Vienna, Austria: IAEA; 2001.
3. Fenech M. The cytokinesis-block micronucleus technique and its application to genotoxicity studies in human populations. *Environ Health Perspect.* 1993;101:101-107.
4. Vral A, Fenech M, Thierens H. The micronucleus assay as a biological dosimeter of vivo ionising radiation exposure. *Mutagenesis.* 2011;26:11-17.
5. Fenech M. The in vitro micronucleus technique. *Mutation Res.* 2000;455:81-95.
6. Fenech M. Cytokinesis-block micronucleus cytome assay. *Nat Protoc.* 2007;2:1084-1104.
7. McCollough CH, Leng S, Yu L, Cody DD, Boone JM, McNitt-Gray MF. CT dose index and patient dose: they are not the same thing. *Radiology.* 2011;259:311-316.

8. Turner AC, Zhang D, Khatonabadi M, et al. The feasibility of patient size-corrected, scanner-independent organ dose estimates for abdominal CT exams. *Med Phys*. 2011;38:820-829.
9. Lee C, Kim KP, Long DJ, Bolch WE. Organ doses for reference pediatric and adolescent patients undergoing computed tomography estimated by Monte Carlo simulation. *Med Phys*. 2012;39:2129-2146.
10. Ding A, Gao Y, Liu H, et al. VirtualDose: a software for reporting organ doses from CT for adult and pediatric patients. *Phys Med Biol*. 2015;60:5601-5625.
11. Fenech M, Chang WP, Kirsch-Volders M, Holland N, Bonassi S, Zeiger E. HUMN project: detailed description of the scoring criteria for the cytokinesis-block micronucleus assay using isolated human lymphocyte cultures. *Mutat Res*. 2003;534:65-75.
12. International Commission on Radiological Protection (ICRP). The 2007 Recommendations of the International Commission on Radiological Protection. ICRP Publication No. 103. *Ann ICRP*. 2007;37:1-332.
13. Rothkamm K, Balroop S, Shekhdar J, Fernie P, Goh V. Leukocyte DNA damage after multi-detector row CT: a quantitative biomarker of low-level radiation exposure. *Radiology*. 2007;242:244-251.
14. International Commission on Radiological Protection (ICRP). Basic anatomical and physiologic data for use in radiological protection: reference values—a report of age- and gender-related differences in the anatomical and physiological characteristics of reference individuals. ICRP Publication No. 89. *Ann ICRP*. 2002;32:5-265.
15. Kanagaraj K, Abdul Syed Basheerudeen S, Tamizh Selvan G, et al. Assessment of dose and DNA damages in individuals exposed to low dose and low dose rate ionizing radiations during computed tomography imaging. *Mutat Res. Genet Toxicol Environ Mutagen*. 2015;789-790:1-6.
16. Stephan G, Schneider K, Panzer W, Walsh L, Oestreicher U. Enhanced yield of chromosome aberrations after CT examinations in paediatric patients. *Int J Radiat Biol*. 2007;83:281-287.
17. Abe Y, Miura T, Yoshida MA, et al. Increase in dicentric chromosome formation after a single CT scan in adults. *Sci Rep*. 2015;5:13882.
18. Shi L, Fujioka K, Sakurai-Ozato N, et al. Chromosomal abnormalities in human lymphocytes after computed tomography scan procedure. *Radiat Res*. 2018;190:424-432.
19. Ait-Ali L, Andreassi MG, Foffa I, Spadoni I, Vano E, Picano E. Cumulative patient effective dose and acute radiation-induced chromosomal DNA damage in children with congenital heart disease. *Heart*. 2010;96:269-274.
20. Li G, Yang P, Hao S, et al. Buccal mucosa cell damage in individuals following dental x-ray examinations. *Sci Rep*. 2018;8:2509.
21. Thierens H, Vral A, Morthier R, Aousalah B, De Ridder L. Cytogenetic monitoring of hospital workers occupationally exposed to ionizing radiation using the micronucleus centromere assay. *Mutagenesis*. 2000;15:245-249.
22. Yang P, Hao S, Gong X, Li G. Cytogenetic biomonitoring in individuals exposed to cone beam CT: comparison among exfoliated buccal mucosa cells of tongue and epithelial gingival cells. *Dentomaxillofac Radiol*. 2017;20160413.
23. Gajski G, Geric M, Orescanin V, Garaj-Vrhovac V. Cytokinesis-block micronucleus cytome assay parameters in peripheral blood lymphocytes of the general population: contribution of age, sex, seasonal variations and lifestyle factors. *Ecotoxicol Environ Saf*. 2018;148:561-570.
24. Cai TJ, Lu X, Tian XL, et al. Effects of age and gender on the baseline and 2 Gy (60)Co gamma-ray-induced nucleoplasmic bridges frequencies in the peripheral blood lymphocytes of Chinese population. *Mutat Res Genet Toxicol Environ Mutagen*. 2018;832-833:29-34.
25. Deric Eker E, Koyuncu H, Şahin NÖ, et al. Determination of genotoxic effects of hookah smoking by micronucleus and chromosome aberration methods. *Medical Sci Monit*. 2016;22:4490-4494.
26. Benassi-Evans B, Fenech M. Chronic alcohol exposure induces genome damage measured using the cytokinesis-block micronucleus cytome assay and aneuploidy in human B lymphoblastoid cell lines. *Mutagenesis*. 2011;26:421-429.

Reprint requests:

Gang Li
Department of Oral and Maxillofacial Radiology
Peking University School and Hospital of Stomatology
#22 Zhongguancun
Nandajie
Hai Dian District
Beijing 100081
China.
Kqgang@bjmu.edu.cn